EXTENSION OF POINT LOMA OUTFALL

In 1983, the State revised the California Ocean Plan and applied body contact standards for bacterial concentrations to beds of giant kelp *(Macrocystis pyrifera)*. This doubled the depth of protected inshore waters from 35 ft (10.7 m) to 70 ft (21.3 m) near the Point Loma ocean outfall (City of San Diego). At the same time, the distance between the outer boundary of the protected area (historical extent of the kelp bed) and the outfall diffuser was reduced from 2.6 km to 1.6 km.

These changes substantially reduced the isolation of the wastefield from areas where the body contact standard must be met and resulted in violations of the standard. An extension of the existing outfall offshore and into deeper water (85-105 m) is a potential way of meeting the bacterial standards in the kelp bed. Increased isolation is achieved by the greater depth of the wastefield in the water column, and by the increased distance between the outfall diffuser and the kelp beds.

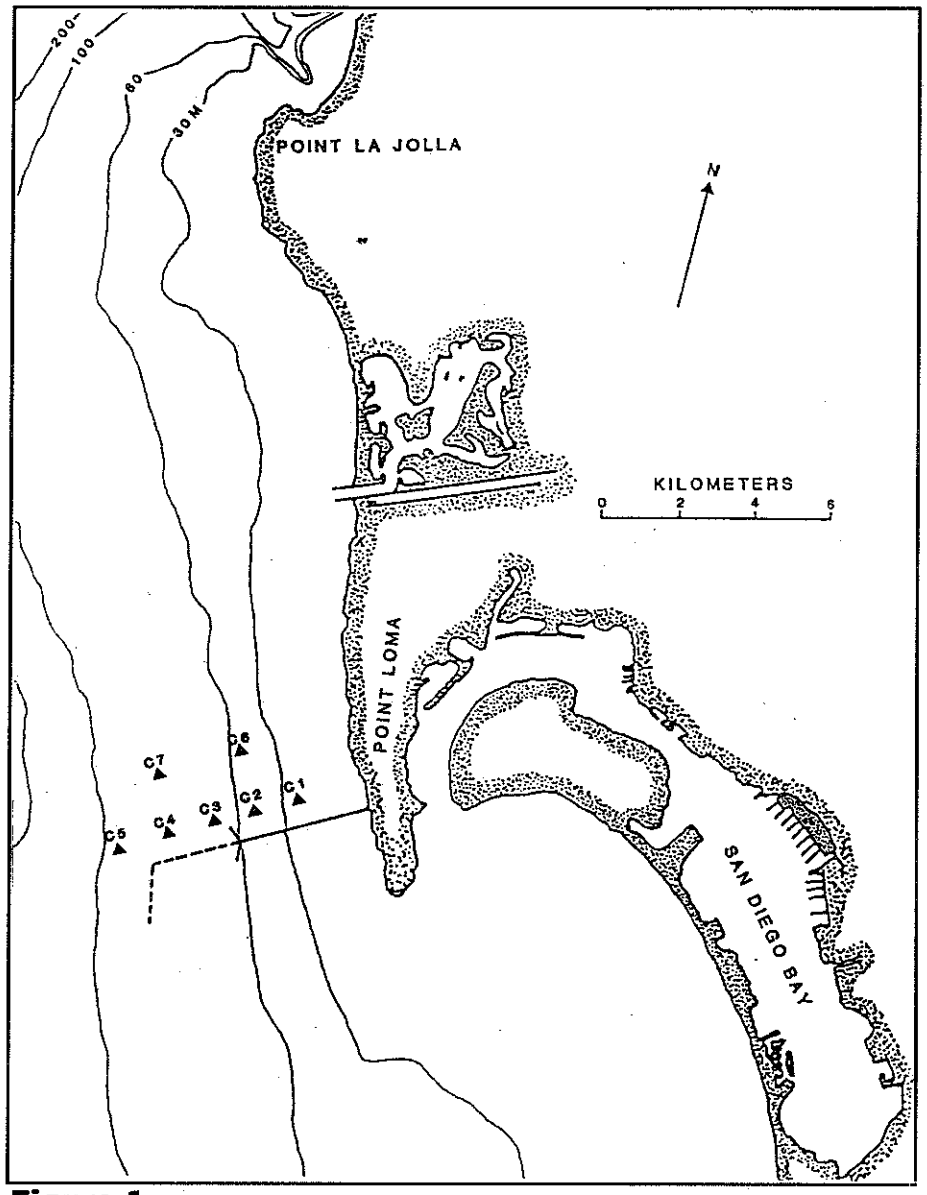

Figure 1
Location of current meter and thermistor moorings (C1-C7) off Point Loma (adapted from Engineering Science, Inc. 1991). Dashed line is potential outfall extension.

Methods

Engineering Science, Inc. subcontracted with SCCWRP to study the feasibility of the proposed extension. We examined the characteristics of water column density stratification and the properties of currents with current meter and thermistor data collected by Engineering Science. The data were collected between March and September 1990 near the Point Loma outfall (Figure 1) by 17 current meters on seven moorings and 51 thermistors on 5 moorings (Figure 2; Appendix 1). The results were incorporated into time-dependent models of initial dilution and transport of wastewater by ocean currents (Appendix 2). Analyses of the oceanographic data and formulation of the simulation models are discussed in Hendricks (1990) and Engineering Science (1991).

Two approaches were used in the simulations. The first approach considered isolation

provided solely by density stratification of the water column. Density stratification suppresses vertical diffusion and advection, and "traps" the diluted wastewater in the water column. If the submerged wastefield is formed sufficiently deep so that its upper boundary always lies below the bottom of the outer edge of the kelp bed, the wastefield will not intrude into the kelp bed. However, because the ocean is a dynamic environment, it is not sufficient to simply ensure that the top of the wastefield lies below the kelp bed depth at the time of formation. Internal tides, internal waves, and slowly varying changes in density structure of the water column can change the depth of the wastefield after its formation. For example, during simulations of a discharge in deep water, vertical excursions of the wastefield of 10 m were common and occasional excursions of 30 m were observed.

The temperature of ambient water at the top of the wastefield at the time of formation was used as a surrogate indicator of water density. This temperature was compared with water temperature measured at the bottom of the outer edge of the kelp bed at later times. If the kelp bed temperature was warmer than the wastefield indicator temperature, the wastefield would not intrude into the kelp bed. If the kelp bed temperature was colder than the wastefield indicator temperature, density stratification of the water column would not prevent an intrusion. The occurrence of an *actual* intrusion, however, depended on ocean currents between the time the wastewater was discharged and when the *potential* intrusion could occur.

Results and Discussion

The fraction of time that a "density window" was "open" for potential intrusions was simulated for seven periods for discharge from a line source (0.05 mgd/ft, or 0.007 m^3/sec-m, of diffuser) in 83 and 95 m of water. We assumed that only wastewater discharged within the preceding five days could result in potential intrusions and that wastewater discharged earlier had been carried out of the area.

The density window was open from 18 to 38% of the time in 83 m, and from 4 to 12% of the time in 95 m (Figure 3). We assumed that data from individual moorings could be used to estimate intrusions at locations between, or offshore from, current meter and thermistor moorings. This assumption is supported by the similarity of the curves for the fraction of time the density window was open as a function of discharge depth (Figure 4).

The actual occurrence of an intrusion during an open density window also depends on ocean currents. During the second phase of the modeling effort, we added time-series measurements of ocean currents and water temperature to a data-driven, time-dependent, three-dimensional model of wastewater transport.

Figure 2
Location of current meters and thermistors on the moorings (adapted from Engineering Science, Inc. 1991). See figure 1 for station locations.

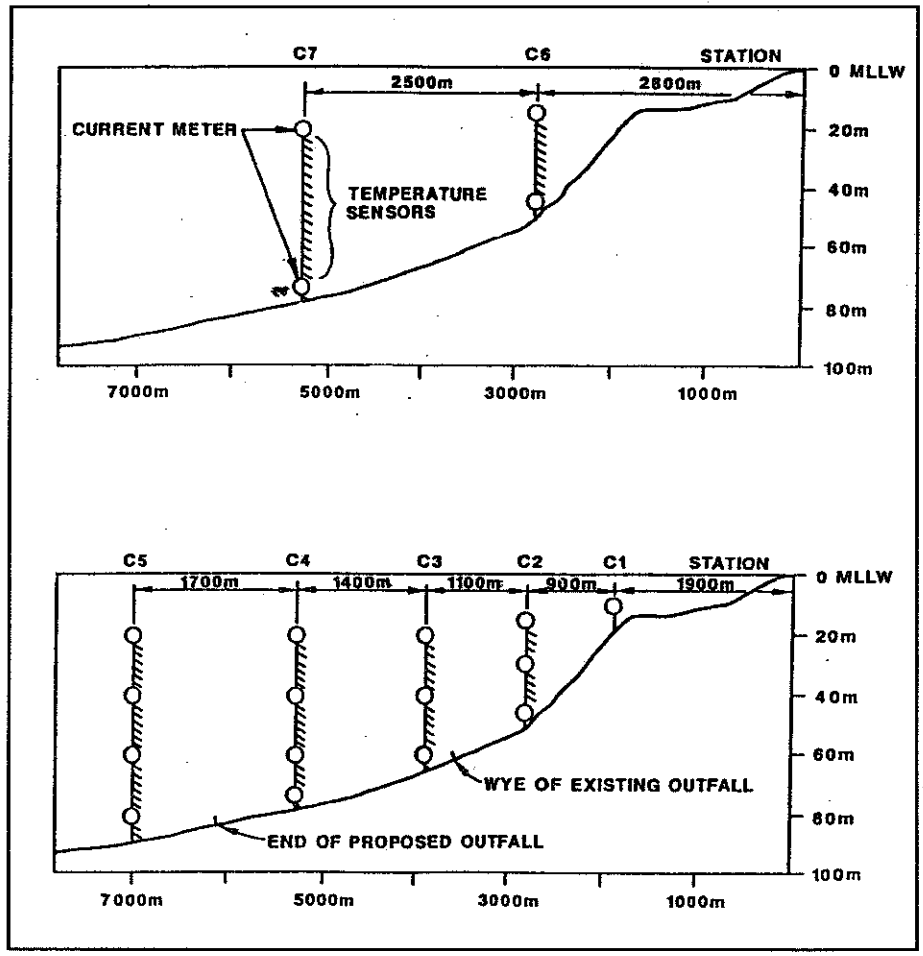

The model predicted that wastewater intrusions into the kelp bed would peak at 15% of the time 1 to 2 km upcoast from an outfall in 83 m of water (Figure 5a). Actual intrusions were predicted for about 40% of potential intrusions. The peak probability was reduced to 7.5% of the time 4 km upcoast from an outfall in 95 m of water (Figure 5b). The increased upcoast displacement for the deeper discharge is the result of increased wastefield transport time from the diffuser to the kelp bed. Actual intrusions were predicted for about 60% of potential intrusions.

The probability of a potential intrusion leading to an actual intrusion was 50% greater for the deeper discharge, i.e., the effectiveness of transport alone in isolating the wastefield from the kelp bed was *reduced* by extending the outfall farther offshore and into deeper water. This somewhat surprising result is probably due to the formation of a deeper wastefield, which leads to an increase in onshore transport by ocean currents at deeper depths (Appendix 1). However, despite increased onshore transport, extending the outfall farther offshore into deeper water reduced the number of actual intrusions.

Intrusion probabilities are not directly convertible into probabilities of regulatory violations. Bathing water standards for total coliform (TC) bacteria require that concentrations not exceed 1000 TC/100 ml more than 20% of the time within a 30-day period. The probability of exceeding the standard depends on the intrusion probability, the distribution of intrusions in a 30-day period, the concentration of TC within the wastefield, and the number of samples collected during the period. For example, let us assume that intrusions occur randomly with a probability of 0.05 in a 30-day period, and that TC concentrations exceed 1000 TC/100 ml when the wastefield is present. If only four samples are collected during a 30-day period, the probability of exceeding the regulatory standard is 0.18 (roughly one out of every five 30-day periods). If 10 samples are collected, the probability falls to about 0.01 (one out of every 100 30-day periods).

These probability estimates may possess considerable uncertainty, particularly for predictions based on the combination of density stratification and wastewater transport. Results of simulated transport were sensitive to the details of cross-shore transport during upwelling and downwelling, including the details associated with internal tides. These processes are not well understood. For example, a shallower isotherm (an indicator

Figure 3
Percent of time the density window was open for discharges in (a) 83 m and (b) 95 m of water from March to September 1990.

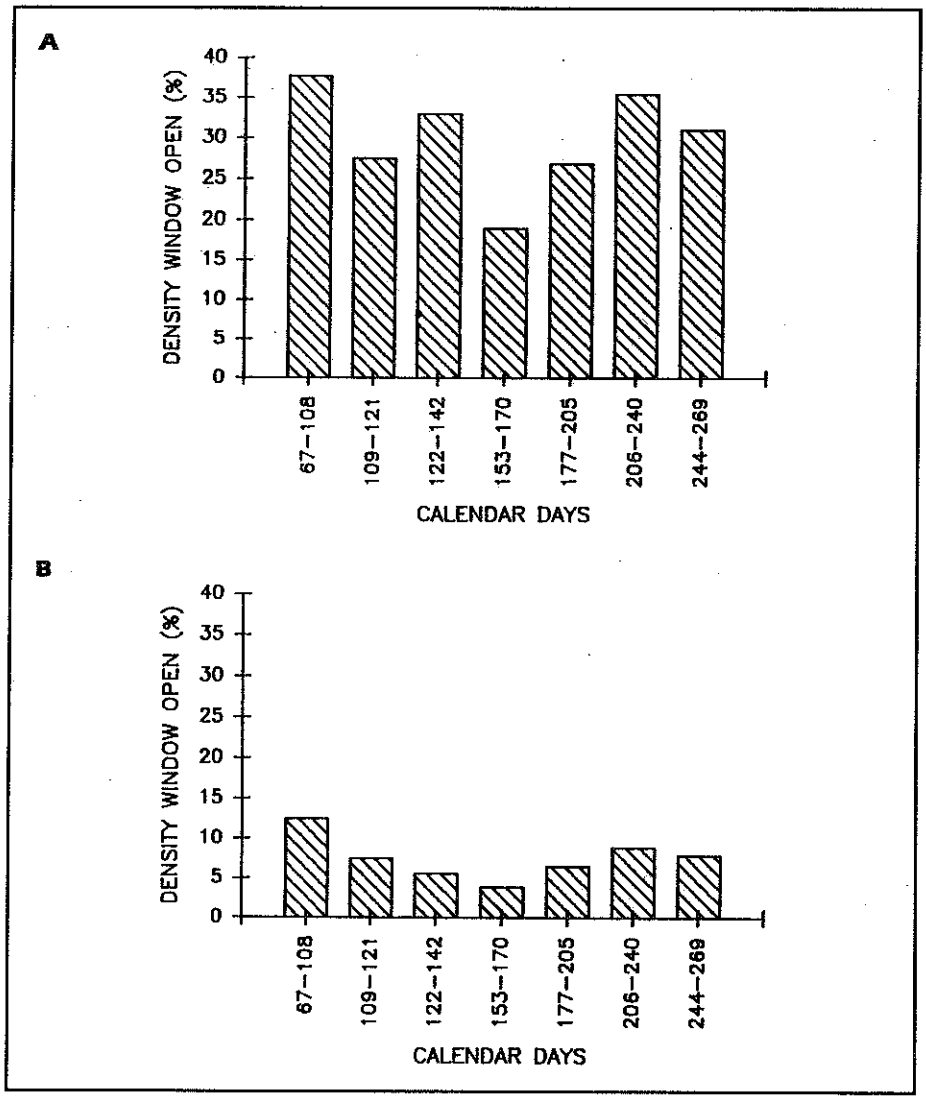

of upwelling) was not always accompanied by onshore flow in waters below that isotherm. This suggests more complex flow patterns for ocean currents than could be resolved from the field measurements.

Similarly, the simulated cross-shore transport associated with a "gravitational collapse" of the wastefield (Wu 1969, Roberts *et al.* 1989a) contributed significantly to onshore transport of wastewater. Gravitational collapse results from relaxation of imbalances between density structures in the wastefield and in the adjacent ambient water, even though average densities in the two regions are equal. However, the measured density stratification in the ocean was much less than in laboratory studies. As a result, frictional effects may be important and the rate of collapse may be much lower than computed in the simulations (e.g., Amen and Maxworthy 1980). In this case, cross-shore transport would be substantially overestimated in the simulation, leading to an overestimate of the intrusion probability.

Estimates based on density considerations are more straight forward and provide an upper bound for intrusion probabilities. The primary uncertainties associated with estimates of potential intrusion probabilities are: 1) changes in the height-of-rise during initial dilution associated with differences between the simulated line-source and the final configuration of the outfall diffuser, 2) lack of oceanographic data for late fall and winter conditions, 3) interannual variability in the oceanographic environment, and 4) neglect of the opposing mechanisms of gravitational collapse of the wastefield and vertical mixing.■

References

- Amen, R. and T. Maxworthy. 1980. The gravitational collapse of a mixed region into a linearly stratified fluid. *J. Fluid Mech.* 96:65-80.
- Engineering Science, Inc. 1991. Point Loma Ocean Plan compliance, ocean outfall extension project report. Volume I - Ocean Measurements project. Report to City of San Diego. Engineering Science, Inc., La Jolla, CA.
- Hendricks, T.J. 1977. Coastal currents. pp. 53-62, *In:* Coastal Water Research Project Annual Report, 1977. Southern California Coastal Water Research Project, Long Beach.
- Hendricks, T.J. 1990. Analysis of cross-shore transport off Point Loma. Report to Engineering Science, Inc., La Jolla, CA. Southern California Coastal Water Research Project, Long Beach. 104 pp.
- Roberts, P.J.W., W.H. Snyder, and D.J. Baumgartner. 1989a. Ocean Outfalls. II: Evolution of submerged wastefield. *J. Hyd. Eng.* 115:26-48.
- Roberts, P.J.W., W.H. Snyder, and D.J. Baumgartner. 1989b. Ocean Outfalls. I: Submerged wastefield formation. *J. Hyd. Eng.* 115:1-25.
- Roberts, P.J.W., W.H. Snyder, and D.J. Baumgartner. 1989c. Ocean Outfalls. III: Effect of diffuser design on submerged wastefield. *J. Hyd. Eng.* 115:49-70.
- Winant, C.D. 1983. Longshore coherence of currents on the Southern California shelf during the summer. *J. Phys. Oceanogr.* 13:54-64.
- Wu, J. 1969. Mixed region collapse with internal wave generation in a density-stratified medium. *J. Fluid Mech.* 65:531-544.

Acknowledgements

Author Terry Hendricks would like to thank Engineering Science, Inc. and the City of San Diego for providing the funding and impetus for the project; Greg McBain, Luciano Mieorin, and Paul Amberg of Engineering Science, Inc. for productive discussions during the study; and Philip Roberts of Georgia Institute of Technology for discussions on modeling initial dilution.

Figure 4

Percent of time the density window was open as a function of the discharge depth for the period of greatest potential for intrusions (3/8/90 to 4/8/90). M4 is the prediction for 83 m (Station C4; Figure 1); M5 is the prediction for 95 m (Station C5).

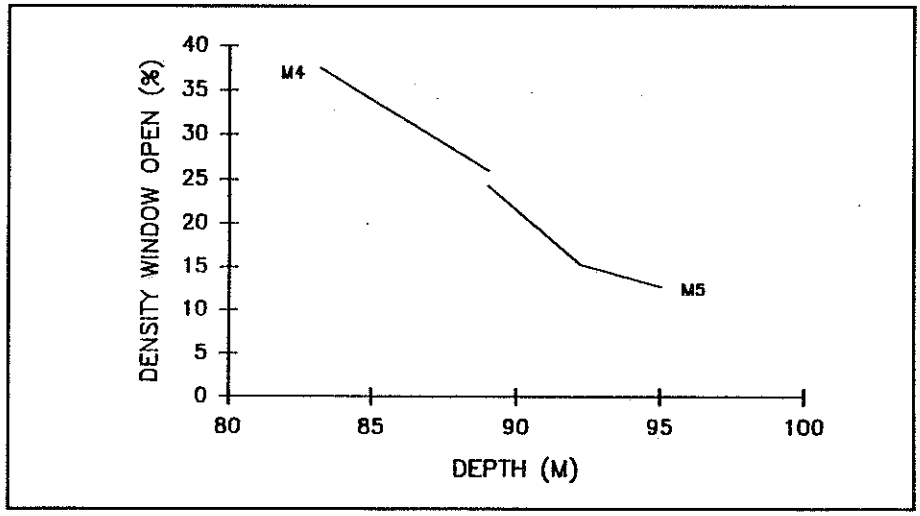

Appendix 1:

Receiving Water Characteristics

Current meter and thermistor data were collected at 30 min intervals between March and October 1990. Fluctuations in the currents and temperature structure of the water column were separated by their temporal properties. A 24.75 hr running-average filter was used to divide the time-series into: 1) net current and current fluctuations that vary more slowly than tidal changes ("subtidal" component) and 2) tidal and higher frequency fluctuations ("tidal" component). Flows associated with subtidal fluctuations were predominantly longshore; the principal axis averaged 351-359° magnetic. Transport associated with tidal fluctuations was roughly isotropic (independent of direction), but with a small longshore enhancement. Transport distances characterizing tidal fluctuations were 1-3 km; distances characterizing subtidal fluctuations were tens of kilometers in the longshore direction.

Net flows at depths greater than 40 m were upcoast and ranged from 1.3 to 4.0 cm/sec depending on the distance offshore. The net flow at 20 m had weaker upcoast transport and ranged from 1.4 to 2.4 cm/sec. Net flows in the cross-shore direction were weakly onshore at a depth of 20 m (-0.1 to 0.8 cm/sec). The tendency for onshore flow increased with depth and peaked at 60 m (0.7 to 1.9 cm/sec). Within a few meters of the bottom, net cross-shore movement was offshore (-0.1 to -1.1 cm/sec).

Although data were collected from a large number of current meters and thermistors, the instruments covered only a fraction of the area around the Point Loma outfall. Previous measurements off San Diego (Hendricks 1977) and 30-80 km upcoast (Winant 1983) indicate coherence length-scales of 30-50 km for the subtidal longshore component of the currents. In this study, the coefficient of determination (r^2) for the subtidal longshore component for moorings 2 km apart ranged from 0.42 to 0.85 (increasing offshore). For vertical separations of 20 m on one mooring, r^2 ranged from 0.35 to 0.79 (increasing offshore). For the longshore component of tidal fluctuations, r^2 ranged from 0.14 to 0.72 for horizontal separations of 2 km, and 0.11 to 0.42 for vertical separations of 20 m on one mooring; r^2 generally increased offshore. The dominant pattern for fluctuations in both frequency ranges was a mode in which changes occurred in the same direction at all depths (barotropic mode).

Correlation length-scales for cross-shore motions were shorter than for longshore motions. In the tidal band, r^2 for horizontal separations of about 2 km typically ranged from 0.16 to 0.66, but fell to 0.003 between the innermost pair of moorings (Figure 1). Cross-shore motions are dominated by top and bottom currents in the opposite direction (baroclinic mode). Coefficients of determination between currents at 20 m and currents near the bottom ranged from 0.07 to 0.23. For fluctuations in the subtidal band, r^2 ranged between 0.13 and 0.62 for cross-shore motions at horizontal separations of about 2 km. For the tidal band, r^2 between the innermost two moorings was 0.03. Coefficients of determination between subtidal fluctuations for a vertical separation of 20 m were 0.01 to 0.14 and the flow tended to be barotropic. The

Figure 5

Probability of intrusion as a function of distance away from an outfall discharging in (a) 83 m of water and (b) 95 m of water. Positive distances are upcoast and negative distances are downcoast.

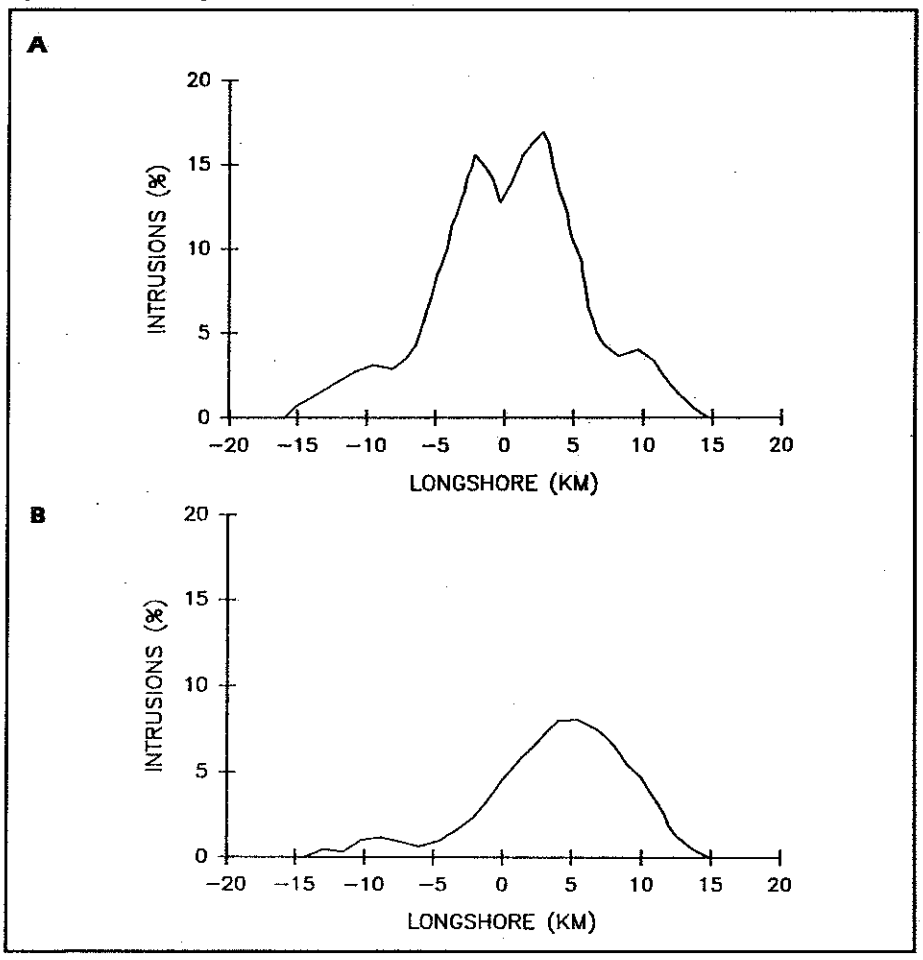

short correlation length-scales for cross-shore motions illustrate the difficulty and uncertainty in estimating cross-shore transport from the current meter data, especially in view of vertical wastefield excursions associated with internal tides and internal waves.

Fluctuations in water temperatures had longer correlation length-scales than did currents, especially for vertical separations (Figure 6). As a result, we could estimate the position of a segment of the wastefield in the water column from temperature data better than we could estimate the cross-shore transport of the same segment from current measurements.

Appendix 2:

Model Formulation

The first stage of modeling simulated formation of a wastefield in the water column after initial dilution. Simultaneous measurements of water column temperature structure and ocean currents in the entrainment region were used to compute characteristics of the wastefield at 30 min intervals. Of particular significance for the intrusion analysis was estimation of ambient water temperature at the depth of the top of the wastefield.

The initial dilution model (TSLINE) was developed from physical model studies by Roberts *et al.* (1989a,b,c), which used a constant density gradient ("linear density profile") in the receiving water. The density gradient in the ocean, however, generally increased with decreasing depth until reaching the pycnocline. The equilibrium depth of the wastefield in the water column was calculated iteratively by assuming a linear density gradient between diffuser port depth and equilibrium depth. The density at each depth was estimated by interpolation from thermistor measurements. Temperature was converted into density using temperature-salinity-density relationships from CTD (conductivity-temperature-depth) data collected on monthly hydrocast surveys.

Once the equilibrium depth of the wastefield was determined, the ambient water temperature at the top of the wastefield ("wastefield temperature") was computed from the average temperature gradient. The depth of the top of the wastefield was estimated using relations in Roberts *et al.* (1989a,b,c) for a line source discharge. In the presence of an increasing temperature gradient with decreasing water depth, the approximations tended to overestimate height-of-rise of the plume, but may have underestimated wastefield temperature.

Ambient water temperature was used as a surrogate indicator of the location of the top of the wastefield in the intrusion analysis and was stored in a time-series (along with other wastefield indicators such as length of each wastefield segment). The wastefield was represented by a collection of individual segments, each of which had a temperature, and hence a position in the water column. At each time step during the *potential* intrusion simulations, the temperature at the bottom of the kelp bed was compared with the temperature of each wastefield segment formed earlier during the simulation. In practice, the comparison was limited to segments formed within the preceding 5 days (earlier segments were assumed to have been carried out of the area). Since the wastefield was either present or absent at a given time, the comparison with wastefield segments for a specific time during the simulation was terminated as soon as a potential intrusion was detected. The probability of a potential intrusion occurring within the simulation area was the total number of potential intrusions during the simulation period divided by the number of time steps during the period.

In the second stage of modeling, the transport of each segment of the wastefield was simulated as it moved away from the diffuser. The first step was to establish the position of each segment in the water column. The cross-shore position at each time step was used to determine the pair of thermistor moorings that bracketed the position. Water temperatures recorded at the two closest thermistor moorings were examined to find the depths that corresponded to wastefield temperature. These depths were used to determine the pair of current meters on each of the two closest moorings that bracketed the depth associated with the wastefield

Figure 6

Temperature fluctuations in the subtidal frequency mode from June to August 1990 at three depths on moorings M2 (Station C2; Figure1) and M6 (Station C6).

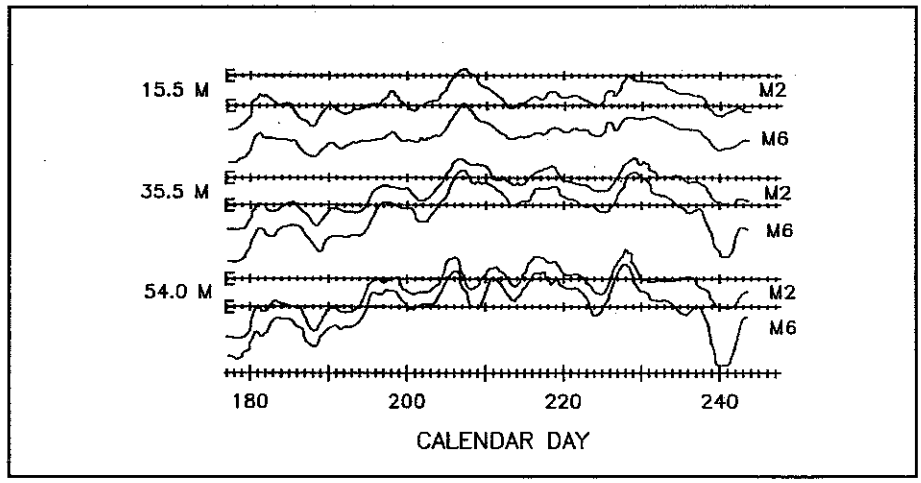

temperature. Velocities measured at the pair of moorings were used to estimate the velocity components at the wastefield depth at each mooring. These were interpolated to estimate the velocity at the location of the wastefield segment. This velocity was used to estimate the position of the segment at the beginning of the next time step. This process was repeated for each wastefield segment at each time-step until the segment moved beyond the boundaries of the simulation area (16 km upcoast and downcoast from the diffuser), or the current meter data were exhausted. If the segment was transported out of the simulation area, it was removed from further computations.

Since measured flows generally had a net onshore movement, the simulated transport eventually moved a wastefield segment onshore. This cannot occur in the real ocean. To prevent this, the depth and position of each wastefield segment was checked at the end of each time step. If the depth of the segment was greater than the water depth at its predicted location, the segment was in deeper water farther offshore. Therefore, the predicted position of the wastefield segment was moved offshore until its depth was equal to the water depth.

An *actual* intrusion occurred whenever a wastewater segment moved inshore of the 25 m isobath (although kelp beds are absent from some sections of the coast). To calculate intrusion probabilities, the coast was divided into 1 km intervals. The fraction of each coastal interval affected by the intrusion was determined from the longshore position of the segment and segment length. For example, if a 1 km coastal interval was included within a wastefield segment, the probability of an intrusion was unity. If the segment only spanned one-quarter of the coastal interval, the intrusion probability was 0.25. The probability of an intrusion within a coastal interval at any given time in the simulation was equal to the sum of the probabilities associated with each wastefield segment at that time. The intrusion probability for the coastal interval for an entire simulation period was equal to the sum of the probabilities for each computation time divided by the number of these times during the period.

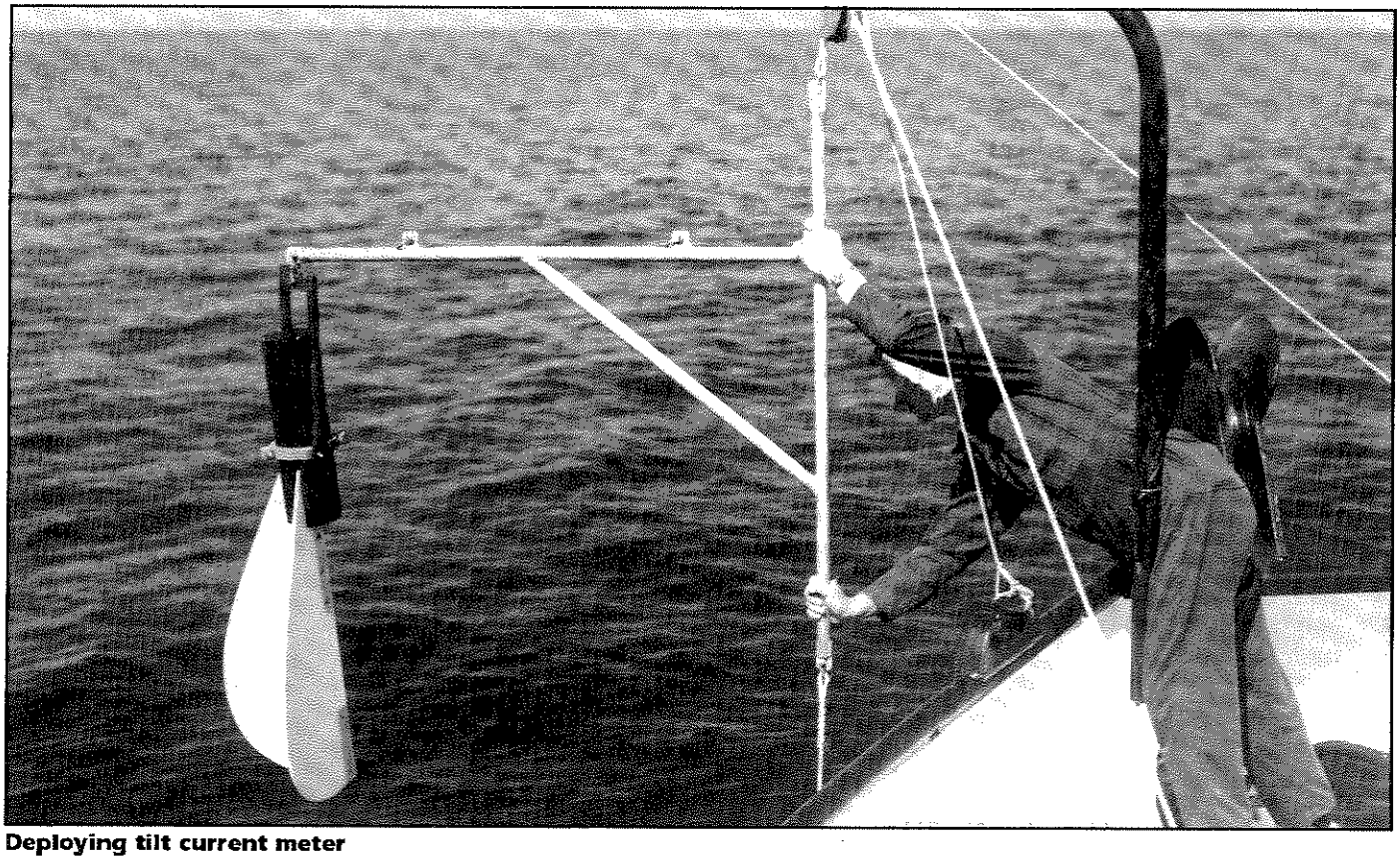

Deploying tilt current meter